Rotation of a Single Molecule Within a Supramolecular Bearing

J. K. Gimzewski,* C. Joachim, R. R. Schlittler, V. Langlais, H. Tang, I. Johannsen

Experimental visualization and verification of a single-molecule rotor operating within a supramolecular bearing is reported. Using a scanning tunneling microscope, single molecules were observed to exist in one of two spatially defined states laterally separated by 0.26 nanometers. One was identified as a rotating state and the other as an immobilized state. Calculations of the energy barrier for rotation of these two states show that it is below the thermal energy at room temperature for the rotating state and above it for the immobilized state.

In recent years, miniaturization of mechanical devices such as gears, bearings, and even motors has been achieved through silicon micromechanics (*1*). However, these devices still have limited lifetimes, and their dimensions are in the tens of micrometers range. Several biological systems use rotary motion, such as flagellar motors (~50 nm in size) (*2*) and molecular motors (~10 nm in size) based on H^+ adenosine triphosphate synthase (*3*). Molecular-based mechanical devices have also been proposed (*4*).

Here, we demonstrate the real-space realization of single-molecule rotors surrounded by like molecules that form a supramolecular bearing. Evidence of their high-speed rotation, driven by thermal energy at room temperature, was obtained by means of scanning tunneling microscopy (STM). The calculated energy barriers for rotation support our experimental observations.

The single-molecule rotors are propeller-shaped units ~1.5 nm in diameter. In the molecular structure of hexa-*tert*-butyl decacyclene (HB-DC), the decacyclene core is equipped with six bulky *t*-butyl legs (Fig. 1). Steric interactions between H atoms on the three outer naphthalene rings twist the molecule with respect to its central benzene ring, endowing it with a propeller form (*5*).

These propeller molecules were deposited on atomically clean Cu(100) surfaces and studied, using STM in ultrahigh vacuum (UHV). At monolayer coverage, the molecules are immobilized by intermolecular steric interactions and form a two-dimensional (2D) van der Waals crystal (Fig. 2). The internal structure of each consists of six lobes arranged in a hexagonal lattice with alternating distances of 0.6 and 0.8 nm between the lobes. From the known dimension of the molecule and from STM-ESQC (elastic scattering quantum chemistry) calculations (*6*), each of the lobes can readily be assigned to a *t*-butyl appendage. Here, the six lobes are used for molecular recognition (*7–9*) and observation of molecular rotation.

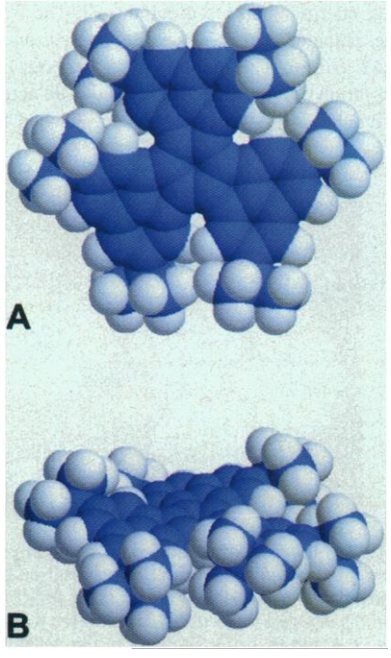

Fig. 1. Top (**A**) and side (**B**) views of models of the molecular structure of hexa-*tert*-butyl decacyclene (HB-DC). The molecule consists of a central conjugated decacyclene core with six *t*-butyl legs attached to its peripheral anthracene components. Atoms of C and H are blue and white, respectively. The *t*-butyl groups are 0.757 nm apart on each naphthalene component and 0.542 nm apart attached to adjacent naphthalene components.

HB-DC adsorbed at submonolayer coverages on Cu(100) exhibits extremely high mobility as a result of the weak adsorption of the H atoms attached to the *t*-butyl legs on the Cu surface. Real-space imaging techniques such as STM are unable to resolve such highly diffusive molecules, because they traverse the tunneling gap at speeds exceeding the response time of the electronic regulation system (*9, 10*).

At coverages of just less than one monolayer, STM images resemble those of the immobilized 2D lattice at full monolayer coverage. However, there is a random array of nanoscopic voids in the layer where molecules have the freedom to choose between several binding sites. In these voids—and only there—we observed images of certain individual molecules with the expected overall dimensions of the six-lobed species but displaying internal contrast in the form of a torus (Fig. 3, B and D). Six-lobed images were always observed if the molecules surrounding them were in the registry of the hexagonal overlayer. In contrast, the toroidal forms were consistently out of registry with the surrounding van der Waals lattice. These

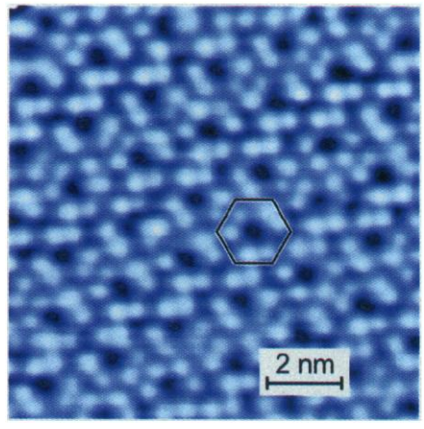

Fig. 2. STM image of an atomically clean Cu(100) surface after exposure to a full monolayer coverage of HB-DC molecules. Each molecule appears as a six-lobed structure in a hexagonal lattice with mean intermolecular separations of 1.78 nm. A subtle difference in the height of the six lobes reflects the propeller conformation and its adaptation to interaction with the substrate. Image area is 11.4 nm by 11.4 nm, recorded with a tunnel voltage of V_t = 1.35 V and tunnel current of i_t = 90 pA. The STM experiments were performed in an UHV STM described elsewhere (*8*). Atomically clean Cu(100) surfaces were prepared by cycles of Ne ion bombardment, followed by annealing at 425°C for 60 min. HB-DC was sublimated from a molecular effusion source at a rate of 0.09 nm/min; the sample temperature was 350°C. Tungsten tips were electrochemically etched, subjected to in situ electron-beam heating and field-ion sharpening using Ne gas at a current of 150 mA. STM images were recorded, using a digital feedback loop data-acquisition system (ECS Ltd., Cambridge, UK).

J. K. Gimzewski, R. R. Schlittler, V. Langlais, IBM Research Division, Zurich Research Laboratory, Säumerstrasse 4, 8803 Rüschlikon, Switzerland. C. Joachim and H. Tang, CEMES-CNRS, 29 rue J. Marvig, Boîte Postale 4347, 31055 Toulouse Cedex, France. I. Johannsen, Risø National Laboratory, Condensed Matter Physics and Chemistry Department, Post Office Box 49, DK-4000 Roskilde, Denmark.

*To whom correspondence should be addressed. E-mail: gim@zurich.ibm.com

observations indicate that, given sufficient space at sites of low symmetry, the molecule rotates at speeds higher than the scan rate used for imaging. This results in a time-averaged image, which reduces the six lobes to a toroidal form.

Two other possibilities exist for the observation of toroidal structures, both of which can be discounted. It is possible that the torus is not a molecule or is a decomposed molecule (*8*), or that the molecular structure is smeared to a torus by lateral diffusion. Figure 3 shows a sequence of images of a toroidal structure, which was observed to exist in one of two states involving a lateral translation of 0.26 nm. A toroidal structure was observed when the molecular rotor was located at a low-symmetry site with respect to the surrounding molecules (Fig. 3, B and D). After lateral translation of the same molecule into a higher-symmetry site (Fig. 3, A and C), the six lobes of the immobilized molecule in its engaged state could be clearly observed. This observation supports the conclusion that an intact molecule exists in a rotational (disengaged) state or immobilized (engaged) state. If the molecule were to exhibit a very rapid translational oscillatory motion, then the dimensions of the toroidal structure would be larger than those of the molecular image in its immobilized state. We confirmed that the overall dimensions of the torus and the six-lobed structures were identical, which allowed us to eliminate this possibility.

These observations permit us to make some statements concerning the nature of the molecular rotor. First, rotation should occur at low-symmetry sites and is controlled by supramolecular interactions of the molecular rotor with a bearing formed by the surrounding molecules. Second, the rotation appears to be driven by thermal energy. Using ESQC coupled with molecular mechanics calculations (ESQC-MM2), we computed the mechanics of the molecular bearing. We considered the supramolecular bearing with the molecular coordinates first extracted from the STM images in Fig. 3, A and B before optimizing the bearing (Fig. 4, A and B). Then, the full atomic conformation of each of the six molecules forming the rotor and bearing was optimized, and the central propeller was rotated by 1° steps in both the engaged and the disengaged state. In the engaged state, a rotational barrier of 117 kJ/mol was obtained. Here, the central HB-DC forms a ratchet in the cavity and, hence, has no significant rotational degree of freedom at room temperature. In the disengaged state, the rotor is first shifted 0.26 nm out of registry with the molecular lattice (Fig. 3). This is sufficient to lower its rotation barrier to 29 kJ/mol, and the central HB-DC is now free to rotate. This is in excellent agreement with our observations. As HB-DC was rotated, the conformation of the *t*-butyl groups in contact was observed to reorient. In addition, we calculated a translation-energy barrier to move the HB-DC from the engaged to the disengaged position of ~42 kJ/mol. This is consistent with our observation of a low rate of lateral shuttle action driven by kT as observed in Fig. 3 when the molecule moves from the engaged to the disengaged state.

Compared to many proposed or synthesized molecular mechanisms (*11–14*), our molecular rotor works in a dry state and appears to be wearless. Its transition from the fixed to the rotating states can be controlled locally by STM tip manipulation (*8*). The mass of the rotor is only 1.33×10^{-24} kg, leading to negligible inertia, and the rotor will stop instantaneously when the external drive is stopped. To examine the time scale of the rotation, we also recorded the tunnel current and its Fourier components up to ~30 kHz, for both their fixed and rotating states. The tunnel-current noise displays a $1/f$ noise characteristic similar to the immobilized molecule, indicating that the motion occurs on a shorter time scale.

The potential energy profile shown in Fig. 4C is highly asymmetric, but periodic in the engaged state. Chemically driven protein motors (*15*) and unimolecular ratchets (*16*) also have asymmetric rotational potentials. These potentials are reminiscent of Feynman's "ratchet and pawl" devised to show that it is not possible to extract unidirectional rotational work from the background thermal noise (*17*). Similar to Maxwell's demon (*18*), the second law of thermodynamics cannot be violated by such macroscopic devices, because work cannot be extracted from background (white) noise (*17*). It has nevertheless been proposed that work can be extracted, using an asymmetric periodic potential, if a secondary colored noise is applied and therefore rectified by the system (*14*). In the spirit

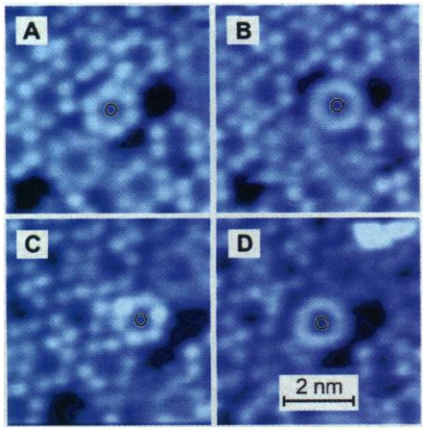

Fig. 3. Sequence of STM images of an atomically clean Cu(100) surface after exposure to a coverage just below one complete monolayer of HB-DC measured in UHV at room temperature. In (**B**) and (**D**) the molecule is imaged as a torus and is in a location where it is not in phase with the overall 2D molecular overlayer (disengaged state). In (**A**) and (**C**), the same molecule is translated by 0.26 nm and imaged as a six-lobed structure in registry with the surrounding molecular layer. Image area is 5.75 nm by 5.75 nm, recorded with a tunnel voltage of $V_t = 0.35$ V and a tunnel current of $i_t = 90$ pA.

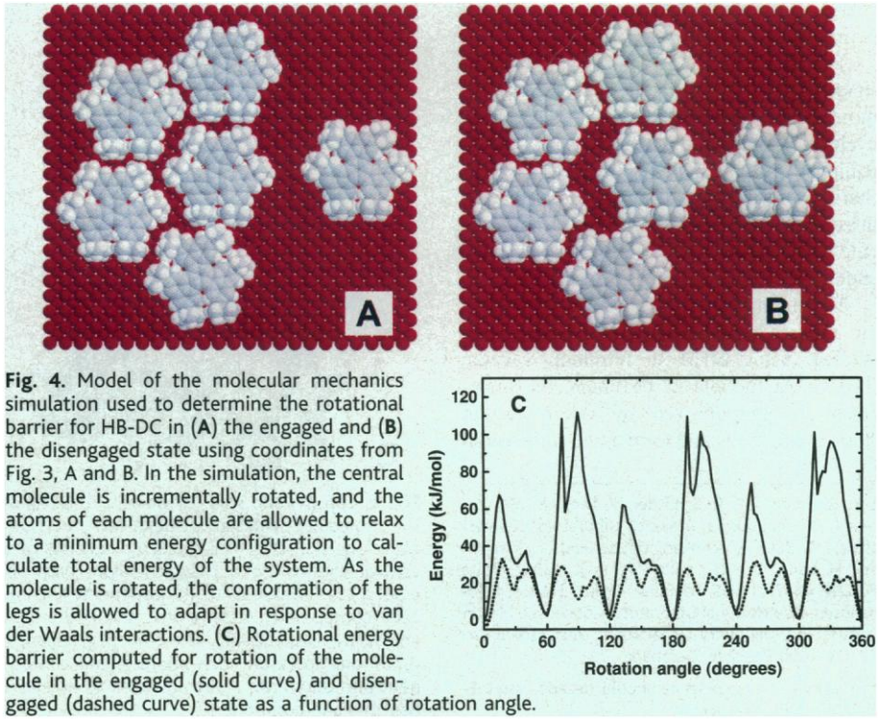

Fig. 4. Model of the molecular mechanics simulation used to determine the rotational barrier for HB-DC in (**A**) the engaged and (**B**) the disengaged state using coordinates from Fig. 3, A and B. In the simulation, the central molecule is incrementally rotated, and the atoms of each molecule are allowed to relax to a minimum energy configuration to calculate total energy of the system. As the molecule is rotated, the conformation of the legs is allowed to adapt in response to van der Waals interactions. (**C**) Rotational energy barrier computed for rotation of the molecule in the engaged (solid curve) and disengaged (dashed curve) state as a function of rotation angle.

of Maxwell (*18*) and Feynman (*19*), devices with nanoscale dimensions may actually approach the limit of the second law of thermodynamics, be they mechanically (*20*) or electrically (*21*) driven. Our results point the way for the creation of such a mechanical "ratchet and pawl" device, although the asymmetric periodic profile in our experiment here may not be sufficiently strong at room temperature to ensure the necessary conditions for a completely unidirectional rotation of the molecular rotor (*17*). The rotor (or the cavity) has to be reengineered to optimize the supramolecular ratchet-bushing interaction. In this case, to drive the rotor unidirectionally by thermal means, an additional input is required to increase the rotor potential energy over the ratchet potential barrier at pseudorandom time intervals (*14, 17*). For example, a tunnel current input on the bearing will inelastically heat the rotor (*22*), thus providing a method to rectify thermal noise.

Our results open the way to fabricate, spatially define, and test recent proposals involving mechanical devices fabricated in molecular structures. They raise interesting questions concerning the fundamentals of mechanics in molecular and supramolecular systems, including the role of thermal noise and the design of molecular devices.

References and Notes

1. R. T. Howe, R. S. Muller, K. J. Gabriel, W. S. N. Trimmer, *IEEE Spectrum* **27**, 29 (1990).
2. H. Noji, R. Yasuda, M. Yoshida, K. Kinosita, *Nature* **386**, 299 (1997); H. Miyata *et al.*, *Biophys. J.* **68**, 286S (1995).
3. A. Ishijima *et al.*, *Biochem. Biophys. Res. Commun.* **199**, 1057 (1995); S. M. Block, *Nature* **386**, 217 (1997).
4. K. E. Drexler, *Nanosystems: Molecular Machinery, Manufacturing, and Computation* (Wiley, New York, 1995); D. H. Robertson, B. I. Dunlap, D. W. Brenner, J. W. Mintmire, C. T. White, *Mater. Res. Soc. Symp. Proc.* **349**, 283 (1994); K. Sohlberg, R. E. Tuzun, B. G. Sumpter, D. W. Nold, *Nanotechnology* **8**, 103 (1997).
5. D. M. Ho and R. A. Pascal Jr., *Chem. Mater.* **5**, 1358 (1993).
6. C. Chavy, C. Joachim, A. Altibelli, *Chem. Phys. Lett.* **214**, 569 (1993).
7. T. A. Jung, R. R. Schlittler, J. K. Gimzewski, *Nature* **386**, 696 (1997).
8. J. K. Gimzewski, T. A. Jung, M. T. Cuberes, R. R. Schlittler, *Surf. Sci.* **386**, 101 (1997).
9. M. T. Cuberes, R. R. Schlitter, T. A. Jung, K. Schaumburg, J. K. Gimzewski, *ibid.* **383**, 37 (1997).
10. S. J. Stanick, M. M. Kamna, P. S. Weiss, *Science* **266**, 99 (1994).
11. P. L. Anelli, N. Spencer, J. F. Stoddart, *J. Am. Chem. Soc.* **113**, 5131 (1991).
12. R. Ballardini *et al.*, *Angew. Chem. Int. Ed. Engl.* **32**, 1301 (1993).
13. A. Livoreil, C. O. Dietrich-Buchecker, J. P. Sauvage, *J. Am. Chem. Soc.* **116**, 9399 (1994).
14. M. O. Magnasco, *Phys. Rev. Lett.* **71**, 1477 (1993).
15. R. D. Astumian and M. Bier, *ibid.* **72**, 1766 (1994).
16. T. R. Kelly, I. Tellitu, J. P. Sestelo, *Angew. Chem. Int. Ed. Engl.* **36**, 1866 (1997).
17. R. D. Astumian, *Science* **276**, 917 (1997).
18. H. S. Leff and A. F. Rex, Eds., *Maxwell's Demon: Entropy, Information and Computing* (Adam Hilger, Bristol, UK, 1990).
19. R. P. Feynman, R. B. Leighton, M. Sands, *The Feynman Lectures on Physics* (Adison-Wesley, Reading, MA, 1966), vol. I, chap. 46.
20. C. Joachim and J. K. Gimzewski, *Proc. IEEE* **86**, 184 1998).
21. A. Aviram and M. A. Ratner, *Chem. Phys. Lett.* **29**, 277 (1974).
22. B. C. Stipe, M. A. Rezaei, W. Ho, *Science* **279**, 1907 (1998).

23. We thank P. Guéret and M. Welland for useful discussions, and A. K. Lay for help in the chemical synthesis. Supported by the European Union ESPRIT project "Nanowires," which is partially funded by the Swiss Federal Office for Education and Science.

24 March 1998; accepted 30 April 1998

Exploiting Chemical Libraries, Structure, and Genomics in the Search for Kinase Inhibitors

Nathanael S. Gray, Lisa Wodicka, Andy-Mark W. H. Thunnissen, Thea C. Norman, Soojin Kwon, F. Hernan Espinoza, David O. Morgan, Georjana Barnes, Sophie LeClerc, Laurent Meijer, Sung-Hou Kim, David J. Lockhart, Peter G. Schultz*

Selective protein kinase inhibitors were developed on the basis of the unexpected binding mode of 2,6,9-trisubstituted purines to the adenosine triphosphate–binding site of the human cyclin-dependent kinase 2 (CDK2). By iterating chemical library synthesis and biological screening, potent inhibitors of the human CDK2–cyclin A kinase complex and of *Saccharomyces cerevisiae* Cdc28p were identified. The structural basis for the binding affinity and selectivity was determined by analysis of a three-dimensional crystal structure of a CDK2-inhibitor complex. The cellular effects of these compounds were characterized in mammalian cells and yeast. In the latter case the effects were characterized on a genome-wide scale by monitoring changes in messenger RNA levels in treated cells with high-density oligonucleotide probe arrays. Purine libraries could provide useful tools for analyzing a variety of signaling and regulatory pathways and may lead to the development of new therapeutics.

Biomedical research has been aided tremendously by three developments: (i) the ability to generate small molecule libraries using combinatorial chemistry methods coupled with high-throughput screening, (ii) the enormous increase in the number of newly identified gene sequences from a host of different organisms, and (iii) the use of structural methods for the detailed characterization of ligand-protein interaction sites that can be exploited for ligand design. Here we applied these methods to the synthesis and characterization of potent, selective inhibitors of protein kinases involved in cell cycle control. The central role that cyclin-dependent kinases (CDKs) play in the timing of cell division and the high incidence of genetic alteration of CDKs or deregulation of CDK inhibitors in a number of cancers make CDKs a promising target for the design of selective inhibitors. Our approach to inhibiting CDKs has been to block the adenosine triphosphate (ATP)–binding site with compounds derived from combinatorial libraries of 2,6,9-trisubstituted purines. This strategy was motivated by the binding mode of the purine olomoucine, which exhibits good selectivity but only moderate inhibition [IC_{50} (50% kinase inhibition) = 7 μM] of a subset of the CDK family of protein kinases (*1*). The orientation of the purine ring of olomoucine within the ATP-binding site of CDK2 is rotated almost 160° relative to that of the adenosine ring of ATP. Thus, it seemed that the introduction of new substituents at the 2, 6, and 9 positions of the purine ring, rather than substituents appended to the ribose, as is normally done, might lead to enhanced binding affinity and selectivity. A combinatorial approach to modifying the purine scaffold could be valuable in the search for potent and selective inhibitors of various cellular processes because of the ubiquitous occurrence of enzymes that use purines, including the estimated 2000 kinases encoded in the human genome.

N. S. Gray, T. C. Norman, S. Kwon, P. G. Schultz, Howard Hughes Medical Institute, University of California, Berkeley, CA 94720, USA. L. Wodicka and D. J. Lockhart, Affymetrix, 3380 Central Expressway, Santa Clara, CA 95051, USA. A.-M. W. H. Thunnissen and S.-H. Kim, Lawrence Berkeley National Laboratory and Department of Chemistry, University of California, Berkeley, CA 94720, USA. F. Hernan Espinoza and D. O. Morgan, Department of Physiology, University of California, San Francisco, CA 94143–0444, USA. G. Barnes, Department of Molecular and Cellular Biology, University of California, Berkeley, CA 94720, USA. S. LeClerc and L. Meijer, CNRS, Station Biologique, 29682 Roscoff, France.

*To whom correspondence should be addressed.